

# Diffraction of particles in free fall

D. Condado<sup>1</sup>, J. L. Díaz-Cruz<sup>1</sup>, A. Rosado<sup>2</sup>, and E. Sadurni<sup>2\*</sup>

<sup>1</sup>*Facultad de Ciencias Físico Matemáticas, Benemérita Universidad Autónoma de Puebla, 72570 Puebla, México and*

<sup>2</sup>*Instituto de Física, Benemérita Universidad Autónoma de Puebla, Apartado Postal J-48, 72570 Puebla, México*

(Dated: December 14, 2024)

The problem of a beam of quantum particles falling through a diffractive screen is studied. The solutions for single and double slits are obtained explicitly when the potential is approximated by a linear function. It is found that the resulting patterns depend on a quasi-time  $\tau$  given by a function of the coordinate along the propagation axis in a classical combination  $z_0 - t^2 F/m$ , while the diffraction effects along transverse axes are due solely to  $m/\hbar$ . The consequences on the precision at which the equivalence principle can be tested are discussed. Realizations with ultra cold neutrons, Bose-Einstein condensates and molecular beams are proposed.

PACS numbers: 03.75.Be, 04.20.Cv, 37.25.+k

## I. INTRODUCTION

Over the last forty years [1], free falling quantum mechanical particles of different kinds [2–8] have been subjected to various types of perturbations with the purpose of testing Einstein's equivalence principle [9–11]. Our aim is to discuss the role of diffraction in such situations. In classical mechanics, two seemingly equivalent statements of our principle can be given separately for the sake of clarity:

1. Under the influence of a gravitational field, different test masses experience the same accelerations and, under the same initial conditions, they undergo equal trajectories.
2. The gravitational and the inertial mass of a body are equal.

Classical mechanics allows to show that principle 2 actually implies 1, due to a cancellation of masses  $m_i = m_g$  in the equations of motion. This principle is further generalized to relativity, when trajectories of different test masses are postulated as geodesics in a background space-time (in agreement with the weak equivalence principle). Any classical deviation from principle 1 using point masses necessarily entails a violation of 2, but such a historically recognized equality between masses [12] has been experimentally tested with great accuracy since the times of Eötvös [13].

It is now well-known [1] that this situation is no longer true when we deal with quantum mechanical wave packets, even in a non-relativistic regime. The explanation in such a scenario is quite simple: Although the Heisenberg equations of motion may not violate 2, different inertial masses  $M_i, m_i$  may produce different diffusivities of wave packets –e.g. gaussians [14]– appearing in combinations  $\hbar/m_i$  or  $\hbar/M_i$  in front of our natural time units.

Thus, even in the absence of a gravitational field, different masses lead to unequal undulatory effects. It is actually easy to show in the non-relativistic limit that the sole contribution to the violation of Galileo's universality of free fall is the difference in such diffusivities.

In this work we treat the problem of a falling particle passing through a diffractive screen of a general nature and we specialize it to single and double slit configurations, see figure 1. The method consists in obtaining a stationary diffraction pattern (i.e. a beam with well defined energy  $E$ ) in the presence of a potential along the axis of propagation ( $z$  axis). This shall relate the corresponding  $z$  coordinate along the fall with a quasi-time and, as expected, it will produce a modified diffraction pattern when compared to those emerging without external fields – or patterns obtained at rest, should we choose a coordinate frame moving with the average position. It will be shown that the quasi-time depends on both the field intensity  $F/m_i$  and the diffusivity  $\hbar/m_i$ .

Structure of this paper: In section II we recall the specific dependence of wave dynamics on mass ratios and Planck's constant in known examples. In section III the diffraction problem in a force field is solved semi classically under reasonable assumptions. In section IV the formal solution of the problem is presented using an expansion in Airy functions and a study of a wave falling near the diffraction plate is given. In section V we discuss beam realizations in nuclear, molecular and atomic physics with an emphasis on the locus of a focal point in diffraction patterns. We conclude briefly in VI.

## II. ON TRAJECTORIES, PROPAGATORS AND INTERFEROMETERS

Several experiments have been carried out to show the effects in question. Quantum bounces of free falling neutrons can have access to the violation of both 1 and 2 using the energy levels of a semi triangular potential well [2–4]. In a simple semi classical calculation –also possible beyond semiclassics using the roots of the Airy function–

\* sadurni@ifuap.buap.mx

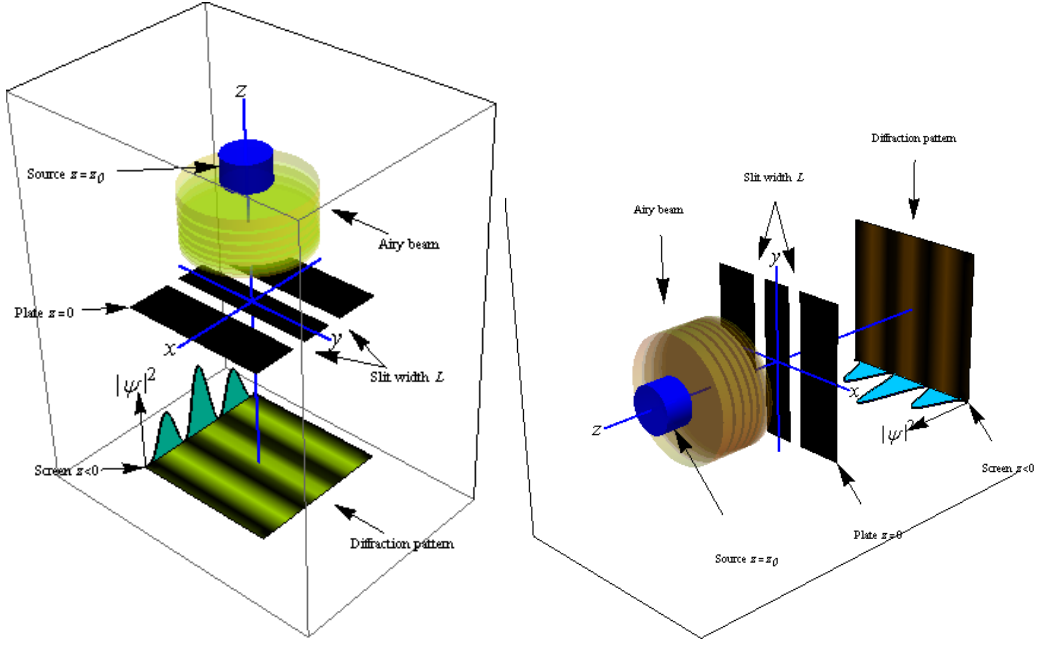


FIG. 1. A diagram of our physical system. The nature of beam sources at  $z = z_0$  (blue) is discussed in section V. The stationary incident wave (yellow) is given by Airy functions, due to gravity. The diffraction plate at  $z = 0$  (black) is the quantum analogue of opaque screens in optics, e.g. Cadmium plates for neutrons. Detectors of adequate resolution are placed at  $z < 0$ .

the Bohr frequency between two stationary states is

$$\frac{E_n - E_{n'}}{\hbar} = \left(\frac{m_i}{\hbar}\right)^{1/3} \left(\frac{F}{m_i}\right)^{2/3} \times \left\{ \left[ \frac{3\pi}{8} (n - 1/4) \right]^{2/3} - \left[ \frac{3\pi}{8} (n' - 1/4) \right]^{2/3} \right\} \quad (1)$$

so that any perturbation capable of driving such transitions would produce a period of oscillation containing

$F/m_i = gm_g/m_i$  and  $\hbar/m_i$ . The quantum dynamics of a more general wave entails the appearance of all Bohr frequencies of the form (1), showing the same dependence for all Fourier components.

For an arbitrary wavepacket falling from the leaning tower of Pisa, the propagator in the  $z$  coordinate and without bounces fulfills the relation [15]

$$K_{\text{field}}(z, z'; t) = K_{\text{free}}(z - Ft^2/2m_i, z'; t) \times \exp \left\{ -i \frac{m_i}{\hbar} \left[ \left( \frac{F}{m_i} \right) zt - \left( \frac{F}{m_i} \right)^2 \frac{t^3}{6} \right] \right\} \quad (2)$$

which gives rise to wave dynamics of the type

$$\psi_{\text{field}}(x, y, z; t) = \exp \left\{ -i \left( \frac{m_i}{\hbar} t \right) \left( \frac{F}{m_i} \right) \left[ z - \left( \frac{F}{m_i} \right) \frac{t^2}{6} \right] \right\} \psi_{\text{free}}(x, y, z - Ft^2/2m_i; t). \quad (3)$$

This means that in a very general picture, the analysis of a single packet boils down to free undulatory effects plus a translation along the path  $z(t) = z - t^2 F/2m_i$  for the density and a translation along  $z(t) = z - t^2 F/6m_i$

for the phase. This is in compliance with (1) and shows that principle 2 breaks down only in a classical fashion, while the factor  $\hbar/m_i$  is the sole responsible for quantum effects and the breakdown of principle 1.

The phase factor in (3), on the other hand, has been exploited in a Mach-Zehnder configuration, where different paths with equal end points would yield the following phase difference

$$\Delta\Phi = \left(\frac{m_i}{\hbar}\right)^2 \left(\frac{F}{m_i}\right) \times A, \quad (4)$$

where  $A$  is the area enclosed by the two paths [16]. One can use the Feynman formulation of the propagator to make the classical action appear in (4), so this calculation is quite general. Once more, the sensitivity in the non-relativistic regime of these experiments is bound to the factors  $F/m_i$  and  $\hbar/m_i$ . Factors depending on proper times along two paths may be achieved if relativistic corrections were included; this can be consulted in [17].

In all, the solutions that we are seeking for in a free falling diffraction setting should exhibit similar field and mass dependences as those in (1, 2) and (3). The surplus is that the resulting pattern shall be static and easier to measure in an experiment, since the only requirement for detection is a good fluorescent screen at various heights  $z$ .

### III. STATIONARY DIFFRACTION PATTERNS IN AN EXTERNAL FIELD

A neutron falling from a source into a diffractive plate at  $z = 0$  is subjected to a force given by  $-V'(z)$ . In the vicinity of the screen, the particle cannot be represented by a plane wave, but instead by the stationary solution of

$$\left[-\frac{\hbar^2}{2m_i}(\partial_x^2 + \partial_z^2) + V(z)\right] \psi(x, z; E) = E\psi(x, z; E), \quad (5)$$

where  $y$  is ignorable if the plate has slits. In a semiclassical approach, if the gravitational potential  $V$  does not have strong variations, we may choose for  $z > 0$  the WKB wave

$$\begin{aligned} \psi(x, z) &= \mathcal{N} \frac{\exp(-i \int_0^z k(\eta) d\eta)}{\sqrt{|k(z)|}}, \\ k(z) &= \sqrt{\left(\frac{2m_i}{\hbar^2}\right) (E - V(z))}. \end{aligned} \quad (6)$$

The singular density at the turning point can be avoided by a better approximation, but in what follows this will be irrelevant, as the WKB phase shall play the important role. Below the screen we have a solution of (5) that depends on both  $x$  and  $z$ . First we absorb the propagating factor with the transformation

$$\tilde{\psi}(x, z) = \psi(x, z) \exp\left(+i \int_0^z k(\eta) d\eta\right). \quad (7)$$

This turns the Schrödinger equation into

$$\begin{aligned} \left[-\frac{\hbar^2}{2m_i} \partial_x^2 + i \frac{\hbar^2 k(z)}{m_i} \partial_z\right] \tilde{\psi}(x, z; E) = \\ \frac{\hbar^2}{2m_i} [\partial_z^2 - ik'(z)] \tilde{\psi}(x, z; E), \end{aligned} \quad (8)$$

and  $k'(z) = im_i V'(z)/\hbar^2 k(z)$ . The semiclassical approach in  $z$  assumes a large  $k(z)$ , a small  $V'(z)$  and small second derivatives of  $\tilde{\psi}$ , which can be established as

$$\left|\tilde{\psi}_{zz} + \frac{im_i V'(z)}{\hbar^2 k(z)} \tilde{\psi}\right| \ll |k(z) \tilde{\psi}|. \quad (9)$$

From here the r.h.s. of (8) can be safely neglected. Then we apply the quasi time transformation [18]

$$\tau(z) = -\int_0^z \frac{m}{\hbar k(\eta)} d\eta, \quad z(\tau) = -\int_0^\tau \frac{\hbar k}{m} dt, \quad (10)$$

which is more than a cosmetic change, since it casts the stationary diffraction problem (5) into an effective one-dimensional time-dependent propagation problem; a clean expression is obtained:

$$\left[-\frac{\hbar^2}{2m_i} \partial_x^2 - i\hbar \partial_\tau\right] \tilde{\psi}(x, z(\tau)) = 0. \quad (11)$$

In the classically allowed region the quasi time is, in principle, a real quantity; we shall see as that the effect of tunneling can be described as well if it becomes complex. The wave shall be obtained by analytic continuation of the solutions into the classically forbidden region.

#### A. One and two slits in a linear potential

The case  $V(z) = Fz$  with  $F > 0$  and  $\tau$  real yields

$$\begin{aligned} k(z) &= \sqrt{\left(\frac{2m_i}{\hbar^2}\right) |E - Fz|}, \\ \tau(z) &= \frac{\sqrt{2m_i}}{F} \left(\sqrt{|E - Fz|} - \sqrt{|E|}\right). \end{aligned} \quad (12)$$

The initial condition is equivalent to the wave coming out of the screen conformed by plates that absorb impinging particles except at some intervals:

$$\psi(x, 0) = \tilde{\psi}(x, z(0)) = \frac{1}{\sqrt{L}} \Theta(L/2 - |x|) \quad (13)$$

for a slit centred at the origin and

$$\begin{aligned}\psi(x, 0) &= \tilde{\psi}(x, z(0)) \\ &= \frac{1}{\sqrt{2L}} [\Theta(L/2 - |x + a|) + \Theta(L/2 - |x - a|)]\end{aligned}\quad (14)$$

for two slits centred at  $x = \pm a$  and  $a > L/2$ . When  $a \rightarrow 0$  one reduces to the other. The general case yields the following solution

$$\begin{aligned}\tilde{\psi}(x, z(\tau)) &= \frac{1}{\sqrt{2L}} e^{i\pi/4} [\mathcal{F}(x_+) + \mathcal{F}(x_-)], \\ x_{\pm} &= \sqrt{\frac{1}{2|\tau(z)|}} (L/2 - a \pm x)\end{aligned}\quad (15)$$

This function seems to depend on  $m_i$  and  $F$  in extra-neous ways, but some physical considerations are in order. When the energy of the emerging beam is controlled by the particle's wavelength or wave number, expression (17) is indeed useful and exhibits new combinations of mass and force. Nevertheless if a particle abandons a radiant source at a certain temperature (e.g. a furnace or

with  $\mathcal{F}$  the exponential Fresnel integral

$$\mathcal{F}(Z) = \int_0^Z e^{ix^2} dx. \quad (16)$$

Evidently  $|\tilde{\psi}| = |\psi|$  in the classically allowed region and the overall semiclassical phase factor adds nothing to the intensity pattern, but the influence of  $F$  makes itself present in the position of maxima and minima in the new quasi time.

For a single slit, a focusing point along the  $z$  axis emerges [19]. The focusing time is such that  $\tau \approx 0.0055 \times m_i L^2 / \hbar$ , where the approximate numerical constant is in fact a root of a transcendental equation involving Fresnel functions. Inverting  $z$  in terms of  $\tau$  using (12) gives an approximation of the focusing height:

$$z_{\text{focus}}(E, L, F/m_i, \hbar/m_i) \approx \frac{E}{F} - \frac{F m_i L^4}{2 \hbar^2} \times \left( 0.055 + \frac{\hbar}{L^2 F} \sqrt{\frac{2|E|}{m_i}} \right)^2. \quad (17)$$

a reactor) we must estimate its initial velocity  $v$  from a statistical rapidity distribution and then select a specific velocity experimentally via a rotating shutter or chopper; this forces to consider  $E = m_i v^2 / 2 + F z_0$  in our non-relativistic experiment. Then (17) is reduced to a more palatable expression in terms of  $\alpha \equiv m_i / F$ ,  $\beta \equiv m_i / \hbar$ :

$$z_{\text{focus}}(v, L, \alpha, \beta) = z_0 + \frac{v^2 \alpha}{2} - \frac{L^4 \beta^2}{2 \alpha} \left[ 0.055 + \frac{\alpha \sqrt{v^2 + 2z_0/\alpha}}{\beta L^2} \right]^2. \quad (18)$$

We should note that the factor in square brackets will depend on  $m_i$  only if the initial height of the drop is  $z_0 \neq 0$ , because the ratio  $\alpha/\beta$  has no inertial mass. We also identify the first two terms in (18) as the classical contribution to the focusing height, while the third term is completely quantum-mechanical. As to the appearance of Planck's constant, only the term affected by the numerical value 0.055 contains it. Special cases can be studied using this formula; for instance, if the particle is shot upwards at zero total energy, i.e.  $z_0 < 0$ , only the quantum term survives. Also, if the energy is properly adjusted, the quantum term can eliminate the classical terms, which can be traced back to the coincidence between the location of the maximum and the classical turning point.

In fig. 2 we show a comparison of probability densities with and without gravitational pull, obtaining the

predicted time deformation due to  $F$ . The effect can be used to control the distance between diffraction peaks as a function of  $\alpha$ . In fig. 3 we show a similar comparison between the near zone pattern emerging from a single slit, showing how the focusing point is moved by  $\alpha$ . The fine details of the pattern near the edges are comparably rich in both cases. In fig. 4 we invert the configuration so as to resemble a fountain of atoms shot upwards; a classical and a tunneling region can be distinguished in these *fleur de lis* patterns.

Finally, we should also note that the time-dependent propagation of wave packets due to a linear potential would offer a very simple alternative for treating this problem, since it would only require a three-dimensional initial condition to be evolved along  $t$  with a gaussian propagator. However, since a diffractive screen is on the way, it would not be advisable to simply guess at the

solution in the immediacy of the rejecting plates, i.e. an arbitrary choice of  $\psi(x, z; t = 0)$  around  $z = 0$ . In contrast, we have presented a method that obtains the solution rigorously in full space.

#### IV. FORMAL SOLUTIONS BEYOND PARAXIALITY

We would like to investigate the solutions of our problem in the region  $|z| \ll \hbar/\sqrt{2m_i E}$ ,  $|x| \gg |z|$  and all values of  $E$ . This corresponds to observation points in the near zone, except for the edges in the case of slits.

In a very general setting, the diffraction kernel can be written in terms known waves. It is important to distinguish the diffraction kernel from the Green's function of the stationary Schrödinger equation, since the former does propagate waves along the  $z$  axis, while the latter cannot be used for diffraction. We start from

$$\left[ -\frac{\hbar^2}{2m_i} (\partial_x^2 + \partial_z^2) + V(z) \right] \psi_{\pm}(x, z) = E\psi_{\pm}(x, z). \quad (19)$$

As before, the upper wave  $\psi_+$  represents a particle falling into the diffractive plate, so (19) admits separable solutions and we choose  $\psi_+(x, z) = \psi_E(z)$  without transversal dependence. This function can be obtained analytically for a number of potentials, so  $\psi_E$  is assumed to be a known solution of

$$\left[ -\frac{\hbar^2}{2m_i} \partial_z^2 + V(z) \right] \psi_E(z) = E\psi_E(z). \quad (20)$$

Now we build  $\psi_-(x, z)$  as a superposition of solutions of (19) at constant energy  $E$ ; from the separability of the equation, we use the products  $e^{ikx}\psi_{\epsilon}(z)$ , which satisfy a dispersion relation  $E = \epsilon + \hbar^2 k^2/2m_i$ :

$$\psi_-(x, z) = \int_{-\infty}^{\infty} dk \quad C(k) e^{ikx} \psi_{\epsilon(k)}(z), \quad (21)$$

$$\epsilon(k) \equiv E - \frac{\hbar^2 k^2}{2m_i}. \quad (22)$$

The coefficients  $C(k)$  are easily determined by direct evaluation of (21) at  $z = 0$ , as we now indicate. Since the l.h.s. of (21) is connected to the wave function coming out of the plate, we write:

$$\psi_-(x, 0) = \phi_E(x) = \int_{-\infty}^{\infty} dk C(k) e^{ikx} \psi_{\epsilon(k)}(z = 0), \quad (23)$$

and  $\phi_E(x)$  is the same wave as  $\psi_E(z = 0)$  blocked in some intervals of  $x$  by the structure of the diffraction

plate. Then, the expression (23) can be Fourier-inverted to give the coefficient

$$C(k) = \frac{1}{2\pi} \int_{-\infty}^{\infty} dx' \left( \frac{\phi_E(x')}{\psi_{\epsilon(k)}(0)} \right) e^{-ikx'}. \quad (24)$$

Finally, (24) is replaced in (21) and the propagated wave is written in terms of a new diffraction kernel

$$\psi_-(x, z) = \int_{-\infty}^{\infty} dx' \phi_E(x') K(x - x', z; E) \quad (25)$$

with

$$K(x - x', z; E) = \int_{-\infty}^{\infty} \frac{dk}{2\pi} \left( \frac{\psi_{\epsilon(k)}(z)}{\psi_{\epsilon(k)}(0)} \right) e^{ik(x-x')}. \quad (26)$$

Our treatment holds for any potential  $V(z)$ . To fix ideas, let us substitute the Airy functions for the choice  $V(z) = Fz$

$$K_{\text{Grav}}(x - x', z; E) = \int_{-\infty}^{\infty} \frac{dk}{2\pi} \left[ \frac{\text{Ai}(\kappa z - \gamma\epsilon(k))}{\text{Ai}(-\gamma\epsilon(k))} \right] \times e^{ik(x-x')}, \quad (27)$$

where  $\kappa = (\hbar^2 F^5)^{1/3}/2m_i$ , and  $\gamma = \kappa/F$ . In (27), any normalization factors accompanying the Airy functions cancel out due to the quotient  $\psi_{\epsilon}(z)/\psi_{\epsilon}(0)$ . This function is itself a solution of the stationary problem with normalization  $\psi(0) = 1$ .

##### A. Wave falling in the near zone

For a single slit, direct integration of (25) using (13) and (27) obtains

$$\psi_-(x, z) = \frac{1}{2\pi i \sqrt{L}} \int_{-\infty}^{\infty} \frac{dk}{k} \left[ \frac{\text{Ai}(\kappa z - \gamma\epsilon(k))}{\text{Ai}(-\gamma\epsilon(k))} \right] \times \left[ e^{ik(x+L/2)} - e^{ik(x-L/2)} \right]. \quad (28)$$

Taylor-expanding the Airy quotient for small  $z$  must yield good results. The simplest way to proceed is to insert in (28) the asymptotic form of the Airy function [20] for large  $k$ :

$$\frac{\text{Ai}(\kappa z - \gamma\epsilon(k))}{\text{Ai}(-\gamma\epsilon(k))} \approx \frac{(-\gamma\epsilon)^{1/4}}{(\kappa z - \gamma\epsilon)^{1/4}} \times \exp \left\{ -\frac{2i}{3} \left[ (\gamma\epsilon - \kappa z)^{3/2} - (\gamma\epsilon)^{3/2} \right] \right\}. \quad (29)$$

When  $z$  is small, the leading correction comes from

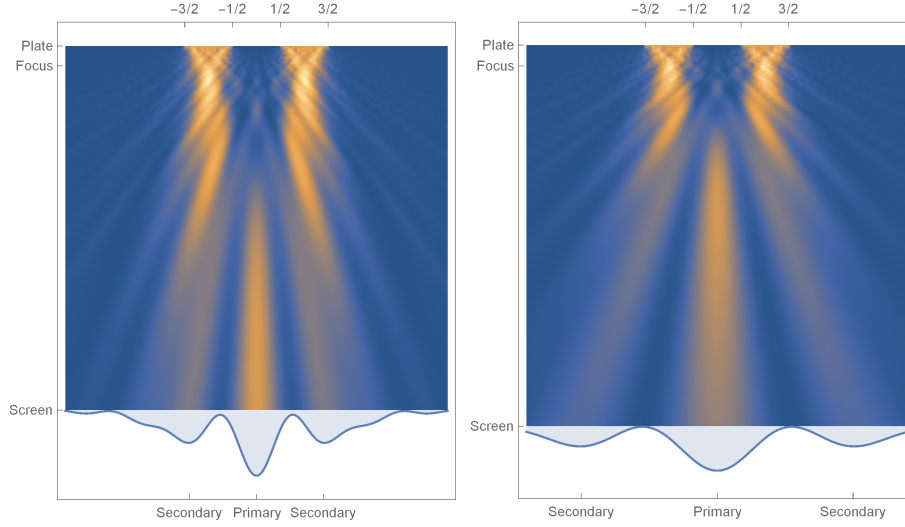


FIG. 2. Left panel: Double slit diffraction pattern with gravitational pull  $F = 5$ ,  $E = 2$ ,  $m_i = m_g = 1$ . Right panel: Same pattern without gravitational pull and constant energy  $E = 2$ . The results show an elongation of the shape; the mark of the free focus point is kept in both panels as point of reference and the detection screen represents the ground. The difference of patterns also shows in the distance between primary and secondary maxima at the screen.

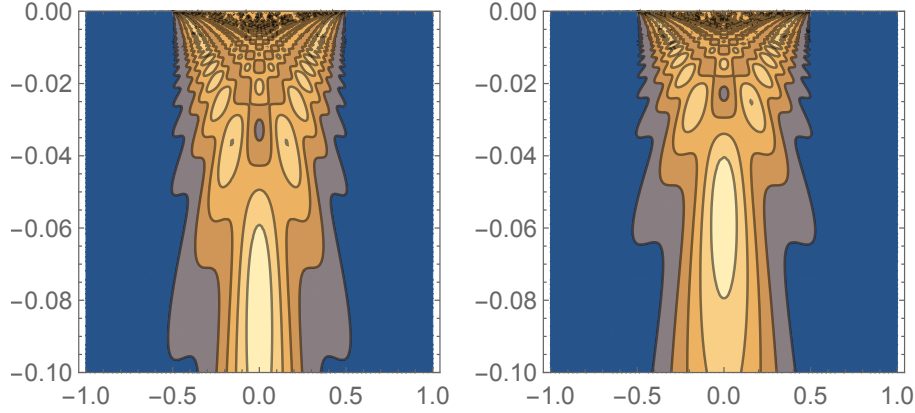


FIG. 3. Left panel: Single slit diffraction pattern in the near zone, with gravitational pull  $F = 5$ ,  $E = 2$ ,  $m_i = m_g = 1$ . The focusing point is  $z \approx -0.09$  in dimensionless variable. Right panel: Same pattern without gravitational pull and same energy  $E = 2$ . Once more we see an elongation with respect to the focus at  $-0.05$ . However, the intricacies due to plate's edges are comparable, showing that interference effects are of the same nature with or without  $F$ .

$$\frac{\text{Ai}(\kappa z - \gamma \epsilon(k))}{\text{Ai}(-\gamma \epsilon(k))} \approx 1 + \frac{\kappa z}{4\gamma \epsilon}. \quad (30)$$

If the particle (atomic cloud, beam of neutrons, etcetera) drops from the slit at negligible velocity, one has  $\epsilon \rightarrow -\hbar^2 k^2 / 2m_i$  and the wave (28) reproduces the initial condition plus regular corrections in  $z$  and  $x$ :

$$\psi_-(x, z) \approx \phi_E(x) + \frac{\kappa z}{8\sqrt{L}} [(x - L/2)^2 - (x + L/2)^2]. \quad (31)$$

where we have used that  $\int_{-\infty}^{\infty} dq e^{iq^3} / q^3 = -i\pi/2$  is the triple antiderivative of the delta distribution evaluated at

1. This gives various correct limit cases such as  $x \rightarrow \infty$  or 0. As promised, the region outside of the paraxial region is well captured by this result. We present the contour plots of  $|\psi_-(x, z)|^2$  in fig.4. No oscillations are observed near the plates.

## V. SENSITIVITY ESTIMATES IN FEASIBLE REALIZATIONS

In the case of a single slit, the position of the focus can be used to infer the values of  $\alpha, \beta$  as functions of the slit width  $L$  and the incident kinetic energy  $E_{\text{kin}}$ . The quantity  $z_{\text{focus}}$  in (18) also shows a sensible dependence on the variations of fundamental constants that can be

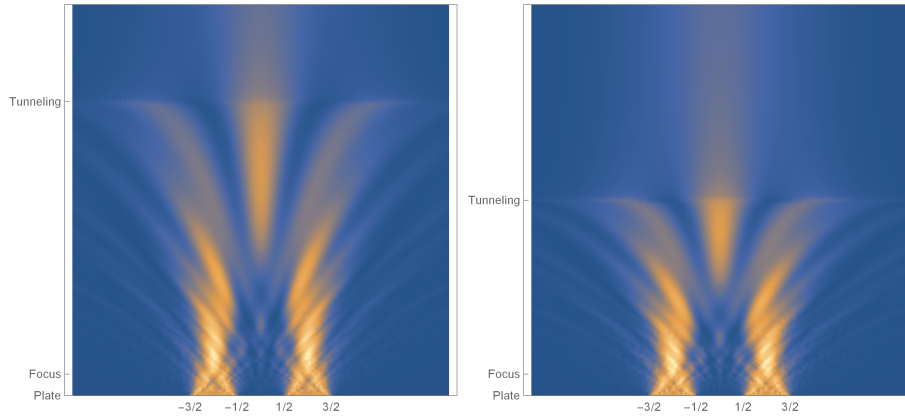


FIG. 4. Left panel: Double slit diffraction pattern with gravitational pull  $F = 4$ . The beam is shot upwards with kinetic energy  $E = 3$ ,  $m_i = m_g = 1$ . The tunneling mark shows the transition to complex quasi time and waves become evanescent, as expected. The curves of constant probability density suffer a bend sideways, producing a fountain-like pattern. Right panel: Same gravitational pull but less kinetic energy  $E = 2$ .

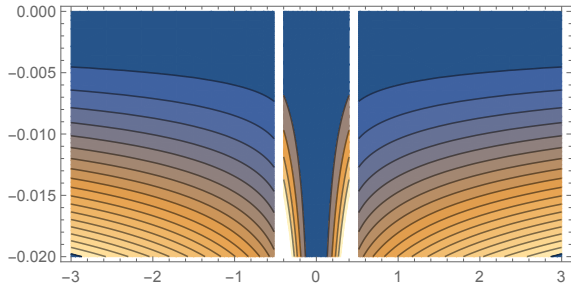


FIG. 5. A contour plot of  $|\psi_-(x, z)|^2$  representing a particle falling from rest, very close to the diffraction plate. As expected, the use of non-paraxial waves produces regular results in the region  $z \ll \sqrt{2m_i E}/\hbar$  and  $|x \pm L/2| \gg z$ .

used to our favour. The idea then is to probe into possible violations of  $m_g = m_i$  for a fixed interferometer, or variations of  $g = F/m_g$  for different positions of the apparatus, i.e. a gravimeter.

We start by writing (18) in terms of its expected value and its possible variation. The constant  $\alpha$  suffers a change due to

$$\tilde{g} = g + \delta g, \quad m_g = m_i + \delta m_g, \quad (32)$$

leading to first order corrections of the form

$$\alpha = \alpha_0(1 + \varepsilon), \quad \alpha_0 = \frac{1}{g}, \quad \varepsilon = -\frac{\delta g}{g} - \frac{\delta m_g}{m_i}. \quad (33)$$

The constant  $\beta = \beta_0$  remains unchanged. When (32) is substituted in

$$z_{\text{focus}} = \frac{\alpha E_{\text{kin}}}{m_i} - \frac{L^4 \beta^2}{2\alpha} \left[ 0.055 + \frac{\alpha}{\beta L^2} \sqrt{\frac{2E_{\text{kin}}}{m_i}} \right]^2 \quad (34)$$

we obtain a first order variation

$$z_{\text{focus}} = z_{\text{focus}}(0) + \varepsilon z'_{\text{focus}}(0) \quad (35)$$

with

$$z_{\text{focus}}(0) = \frac{\alpha_0 E_{\text{kin}}}{m_i} - \frac{L^4 \beta_0^2}{2\alpha_0} \left[ 0.055 + \frac{\alpha_0}{\beta_0 L^2} \sqrt{\frac{2E_{\text{kin}}}{m_i}} \right]^2 \quad (36)$$

and a sensitivity factor

$$z'_{\text{focus}}(0) = (0.055)^2 \times \frac{L^4 \beta_0^2}{2\alpha_0}. \quad (37)$$

This sensitivity factor is independent of the incident kinetic energy of the beam. It is extremely sensitive to the slit width due to the fourth power of  $L$  and it is of a purely quantum-mechanical nature due to  $\beta_0$ . In the absence of gravity,  $g \rightarrow 0$ , this factor also disappears. With (36) and (37) we may give some predictions depending on various beam realizations as we now discuss.

### A. Beam realizations

In table I we include some numerical values of the focusing point  $z'_{\text{focus}}(0)$  and the factor  $z'_{\text{focus}}(0)$  for several values of masses and kinetic energies. The goal is to achieve focusing lengths and sensitivity factors in the same order of magnitude and in mesoscopic dimensions. In nuclear physics, thermal neutrons were proposed long ago in connection with quantum mechanical diffraction and the so-called diffraction in time [21]. This proposal lied among other successful experiments [22–24] which, however, did not involve focusing points. It is interesting to find that Goldemberg and Nussenzveig [25] already studied the possibility of observing diffractive effects,

TABLE I. Beam realizations in different energy scales, the resulting focusing points  $z_{\text{focus}}(0)$  and the corresponding energy-independent sensitivity factors  $z'_{\text{focus}}(0)$ .

	Type	T ( °K)	$L^*$ (m)	$E_{\text{kin}}$ (eV)	$z_{\text{focus}}(0)$ (m)	$z'_{\text{focus}}(0)$ (m)
n	Nuclear	–	$1 \times 10^{-3}$	$3.00 \times 10^{-7}$	$-10.34^{\text{a}}$	3.73
		20		$2.58 \times 10^{-3}$	$-6.17 \times 10^5$	
		300		$3.87 \times 10^{-2}$	$-2.38 \times 10^3$	
NH <sub>3</sub>	Molecular	77	$1 \times 10^{-5}$	$9.95 \times 10^{-3}$	$-0.49$	$1.07 \times 10^{-5}^{\text{b}}$
		300		$3.87 \times 10^{-2}$	$-0.98$	
		1200		$1.54 \times 10^{-1}$	$-1.96$	
Cs	Atomic	1	$1 \times 10^{-4}$	$8.61 \times 10^{-5}$	$-19.51$	6.59
Rb	BEC	$1.7 \times 10^{-7}$	$1 \times 10^{-4}$	$4.28 \times 10^{-11}^{\text{c}}$	$-2.72$	2.71
K	BEC	$5.0 \times 10^{-7}$	$1 \times 10^{-4}$	$4.28 \times 10^{-11}^{\text{c}}$	$-0.57$	0.56

<sup>a</sup> Optimal value, experimentally plausible.

<sup>b</sup> Decreases sensitivity.

<sup>c</sup> Only the free fall energy is considered.

reaching the conclusion that not even 20°K neutrons would allow clean results. Current technology [26, 27] ensures the existence of 300 neV neutrons that may improve dramatically the resolution of diffraction patterns and with this, our gravimeter. The corresponding wavelength reaches up to 50nm, which is smaller than our proposed aperture value  $L^* = 1$  mm, therefore validating the use of a paraxial approximation in our calculations. To our knowledge, this has not been realized yet and, according to our table, this would be the most promising possibility.

In the molecular domain, a beam of ammonia can be produced at several temperatures, ranging from cryogenic environments [28] at 77°K to room temperature and even hot effusion (Knudsen) cells at 1200°K [29]. To compute the incident kinetic energy, we use the  $v_{\text{rms}}$  value obtained from a Maxwellian distribution leading to the typical  $E_{\text{kin}} = 3K_{\text{B}}T/2$  which, according to historical sources [30], induces only 5.5 % of error. Although the numbers for the focusing point reported in our table are encouraging, the sensitivity factor is very small. There is also a caveat concerning the internal structure of these objects [31]; here we have neglected their shape and its influence in transmission peaks through a single slit [32].

A beam of Caesium atoms for atomic clocks represents another interesting possibility. Old standards [33] already suggested beam temperatures of few kelvins. Using a conservative figure of 1°K, our formula yields  $\sim 20$  m for focusing distance and the sensitivity factor is in a similar order of magnitude, which is acceptable. Previous pedagogical realizations with Potassium atoms and high temperature ovens [34] could not spot the near zone effect of focusing.

Finally, we have BECs (Bose-Einstein Condensates), which have been used for gravimetric purposes before. High resolution of the atomic cloud is required [35]. The computation of the incident kinetic energy involves two contributions: the energy acquired in the fall from rest with a time of flight  $\sim 10$  ms and the  $v_{\text{rms}}$  intrinsic to the cloud, obtained from the Bose-Einstein distribution.

Even in this short time of flight, the calculation yields a stronger contribution from the fall, given that a 170 nK Rubidium cloud has a thermal  $\lambda = h/\sqrt{2\pi m K_{\text{B}} T}$  and therefore a negligible  $E_{\text{gas}} \sim 1.4 \times 10^{-11}$  eV. A similar result holds for a 500 nK Potassium cloud.

## VI. CONCLUSIONS

We have calculated the deformation effect on diffraction patterns due to external fields, both in semiclassical and fully quantum-mechanical regimes. The relevant effects are of the same nature, namely, that the classical trajectory governs the average of the packet in a new coordinate akin to a classical trajectory. It is worth to mention that this was done without using Ehrenfest's theorem, circumventing the lack of normalizability of the wave. As a result the sensitivity to the violation of 2 is similar to the classical one. The other effect, i.e. the violation of 1, could be pinned down to a direct correlation between transverse interference effects (such as diffraction in the  $x$  coordinate) and the evolution along the fall (quasi-time in  $z$ ). This was done by identifying the field and mass dependences of the global maximum position in the case of a single slit pattern, and a field and mass dependence of the distance between maxima in a ground-based screen in the case of a double slit.

One could argue that this kind of behaviour should also be observable in free falling gaussians distributed transversally to the falling motion, since their diffusivity is already mass-dependent. However, keeping track of a gaussian's width along the fall is not as advantageous as having a well defined point of reference. We took advantage of a peculiar focusing effect [19, 21] produced by slits, in order to spot accurately the position of the global maximum as the reference point. Then we studied its dependence on  $m_i, m_g, E$  and  $F$ . From this study we were able to suggest experiments in nuclear, atomic and molecular realizations with a twofold purpose: fundamental tests and gravimetry.

## ACKNOWLEDGMENTS

The authors are pleased to thank CONACYT and Sistema Nacional de Investigadores for financial support.

- 
- [1] R. Colella, A. Overhauser, and S. Werner, Observation of Gravitationally Induced Quantum Interference, *Phys. Rev. Lett.* 34 (1975), 1472
  - [2] V. V. Nesvizhevsky, A. K. Petukhov, H. G. Börner, et al. Study of the neutron quantum states in the gravity field, *Eur. Phys. J. C*, 40:4 (2005), 479–491
  - [3] V. V. Nesvizhevsky, H. G. Börner, A. M. Gagarski et al. Measurement of quantum states of neutrons in the Earths gravitational field, *Phys. Rev. D* 67 (2003), 102002
  - [4] J. Hansson, D. Olevik, C. Türk, and H. Wiklund, *Phys. Rev. D* 68 (2003), 108701
  - [5] J. Bateman, S. Nimmrichter, K. Hornberger and H. Ulbricht, Near-field interferometry of a free-falling nanoparticle from a point-like source, *Nature Communications* 5 (2014), 4788 DOI:10.1038/ncomms5788
  - [6] D N Aguilera et al., STE-QUEST test of the universality of free fall using cold atom interferometry, *Class. Quantum Grav.* 31 (2014), 115010
  - [7] H. Muntinga et al., Interferometry with Bose-Einstein Condensates in Microgravity, *Phys. Rev. Lett.* 110 (2013), 093602
  - [8] T. van Zoest et al., Bose-Einstein Condensation in Microgravity, *Science* 328 (2010), 1540.
  - [9] M. P. Haugen and C. Lämmerzahl, *Principles of Equivalence: Their Role in Gravitation Physics and Experiments that Test Them*. Springer (2001)
  - [10] J. L. Synge, *Relativity: The General Theory*, North-Holland Publishing, Amsterdam (1960)
  - [11] R. M. Wald, *General Relativity*, The University of Chicago Press (1984)
  - [12] S. Drake, *Galileo at Work: His Scientific Biography* (Facsim. ed.) Dover, Mineola N.Y. (2003)
  - [13] R. v. Eötvös, *Mathematische und naturwissenschaftliche Berichte aus Ungarn* 8 (1890), 65
  - [14] W. P. Schleich, *Quantum optics in Phase Space*, Chap. 9 Wave Packet Dynamics, WILEY-VCH Berlin (2001)
  - [15] C. Grosche and F. Steiner, *Handbook of Feynman Path Integrals*, Springer (1998)
  - [16] S. Chiow, T. Kovachy, H.-C. Chien, and M. A. Kasevich, 102/hk Large Area Atom Interferometers, *Phys. Rev. Lett.* 107 (2011), 130403
  - [17] D. M. Greenberger, Inadequacy of the Usual Galilean Transformation in Quantum Mechanics, *Phys. Rev. Lett.* 87 (2001), 100405
  - [18] This variable corresponds to the classical time of flight at a given height  $z$ , but since we are dealing with a stationary problem, it does not correspond to time  $t$ .
  - [19] W. B. Case, E. Sadurní, and W. P. Schleich, A diffractive mechanism of focusing, *Optics Express* 20:25 (2012), 27253–27262
  - [20] NIST, *Handbook of Mathematical Functions* (2012). Online at <http://dlmf.nist.gov>
  - [21] M. Moshinsky, Diffraction in Time, *Phys. Rev.* 88 (1952), 625.
  - [22] A.W. Overhauser and R. Colella, Experimental test of gravitationally induced quantum interference, *Phys. Rev. Lett.* 33 (1974), 1237.
  - [23] A.W. McReynolds, Gravitational acceleration of neutrons, *Phys. Rev.* 83 (1951), 172.
  - [24] V. O. de Haan, J. Plomp, A. A. van Well, M. T. Rekveldt, Y. H. Hasegawa, R. M. Dalgliesh and N. J. Steinke, Measurement of gravitation-induced quantum interference for neutrons in a spin-echo spectrometer, *Phys. Rev. A* 89 (2014), 063611.
  - [25] J. Goldemberg and H. M. Nussenzveig, On the possibility of experimental observation of diffraction in time effects, *Rev. Mex. Fis.* 6 (3) (1952) 117–126.
  - [26] G. Bison, M. Daum, K. Kirch, et al. Comparison of ultracold neutron sources for fundamental physics measurements, *Phys. Rev. C* 95 (2017), 045503.
  - [27] R. Golub, D. Richardson, and S. Lamoreaux, *Ultra-Cold Neutrons* (Adam Hilger, Bristol, Philadelphia, and New York, 1991).
  - [28] S. Truppe, M. Hambach, S. M. Skoff, N. E. Bulleid, J. S. Bumby, R. J. Hendricks, E. A. Hinds, B. E. Sauer and M. R. Tarbutt, A buffer gas beam source for short, intense and slow molecular pulses, *Journal of Modern Optics*, 65:5–6 (2018), 648–656, DOI:10.1080/09500340.2017.1384516.
  - [29] <https://www.svta.com/high-temperature-effusion-cell>
  - [30] D. R. Olander, R. H. Jones, and W. J. Siekhaus, Molecular Beam Sources Fabricated from Multichannel Arrays. IV. Speed Distribution in the Centerline Beam, *Journal of Applied Physics* 41 (1970), 4388; <https://doi.org/10.1063/1.1658472>
  - [31] B. Brezger, M. Arndt and A. Zeilinger, Concepts for near-field interferometers with large molecules, *J. Opt. B: Quantum Semiclass. Opt.* 5 (2003), S82–S89
  - [32] B. W. Shore, P. Dömötör, E. Sadurní, G. Süssmann and W. P. Schleich, Scattering of a particle with internal structure from a single slit, *New J. Phys.* 17 (2015), 013046
  - [33] D. J. Wineland, The Cesium beam frequency standard – prospects for the future, *Metrologia* 13 (1977) 121. <https://tf.nist.gov/general/pdf/1815.pdf>
  - [34] J. A. Leavitt and F. A. Bills, Single-Slit Diffraction Pattern of a Thermal Atomic Potassium Beam, *American Journal of Physics* 37, 905 (1969); <https://doi.org/10.1119/1.1975924>
  - [35] T. Gericke, P. Würtz, D. Reitz, T. Langen and H. Ott, High-resolution scanning electron microscopy of an ultracold quantum gas, *Nature Physics* 4 (2008), 949–953.